

Quantum localized modes in capacitively coupled Josephson junctions

R. A. PINTO^(a) and S. FLACH

Max-Planck-Institut für Physik komplexer Systeme - Nöthnitzer Str. 38, 01187 Dresden, Germany

received 25 May 2007; accepted in final form 25 July 2007
published online 8 August 2007

PACS 63.20.Pw – Localized modes
PACS 74.50.+r – Tunneling phenomena; point contacts, weak links, Josephson effects
PACS 63.20.Ry – Anharmonic lattice modes

Abstract – We consider the quantum dynamics of excitations in a system of two capacitively coupled Josephson junctions. Quantum breather states are found in the middle of the energy spectrum of the confined nonescaping states of the system. They are characterized by a strong excitation of one junction. These states perform slow tunneling motion from one junction to the other, while keeping their coherent nature. The tunneling time sensitively depends on the initial excitation energy. By using an external bias as a control parameter, the tunneling time can be varied with respect to the escape time and the experimentally limited coherence time. Thus, one can control the flow of quantum excitations between the two junctions.

Copyright © EPLA, 2007

Josephson junctions are the subject of extensive studies in quantum information experiments because they possess two attractive properties: they are nonlinear devices, and also show macroscopic quantum behavior [1–3]. The dynamics of a biased Josephson junction (JJ) is analogous to the dynamics of a particle with a mass proportional to the junction capacitance C_J , moving on a tilted washboard potential

$$U(\varphi) = -I_c \frac{\Phi_0}{2\pi} \cos \varphi - I_b \varphi \frac{\Phi_0}{2\pi}, \quad (1)$$

which is sketched in fig. 1b. Here φ is the phase difference between the macroscopic wave functions in both superconducting electrodes of the junction, I_c is the critical current of the junction, and $\Phi_0 = h/2e$ the flux quantum. When the energy of the particle is large enough to overcome the barrier ΔU (that depends on the bias current I_b) it escapes and moves down the potential, switching the junction into a resistive state with a nonzero voltage proportional to $\dot{\varphi}$. Quantization of the system leads to discrete energy levels inside the wells in the potential, which are nonequidistant because of the anharmonicity. Note that even if there is not enough energy to classically overcome the barrier, the particle may perform a quantum escape and tunnel outside the well, thus switching the junction into the resistive state [1]. Thus each state inside the well is

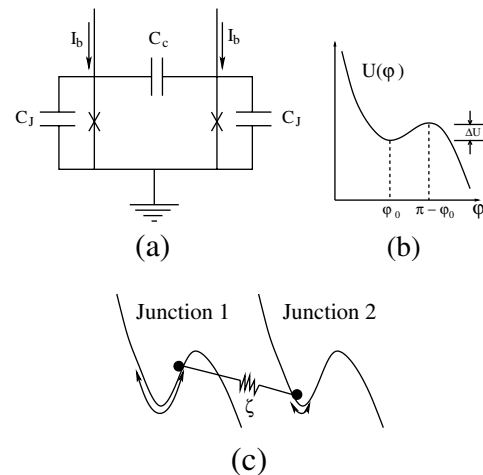


Fig. 1: (a) Circuit diagram for two ideal capacitively coupled JJs. (b) Sketch of the washboard potential for a single current-biased JJ. (c) Sketch of a breather solution in the classical dynamics of the system.

characterized by a bias and a state-dependent inverse lifetime, or escape rate.

Progress on manipulation of quantum JJs includes spectroscopic analysis, better isolation schemes, and simultaneous measurement techniques [2–7], and paves the way for using them as JJ qubits in arrays for experiments on processing quantum information. Typically the

^(a)E-mail: pinto@mpipks-dresden.mpg.de

first two or three quantum levels of one junction are used as quantum bits. Since the levels are nonequidistant, they can be separately excited by applying microwave pulses.

So far, the studies on JJ qubits focused on low-energy excitations involving the first few energy levels of the junctions. Larger energies in the quantum dynamics of JJs give rise to new phenomena that can be observed by using the already developed techniques for quantum information experiments. For instance, it was suggested that Josephson junctions operating at higher energies may be used for experiments on quantum chaos [8–10]. Another phenomenon is the excitation of quantum breathers (QB) [11–13], which are nearly degenerate many-quanta bound states in anharmonic lattices. When such states are excited, the outcome is a spatially localized excitation with a very long time to tunnel from one lattice site to another. So far the direct observation of this kind of excitations evolving in time has not been reported. Up to date evidences of QB excitations were obtained spectroscopically in molecules and solids [14–23].

In this work we consider large energy excitations in a system of two capacitively coupled JJs [24–26]. We study the time evolution of states when initially only one of the junctions was excited. In the low-energy sector such a state will lead to a beating with a beating time depending solely on the strength of the capacitive coupling. For larger excitation energies the states perform slow tunneling motion, where the tunneling time sensitively depends on the initial energy, in contrast to the low-energy beating time. We calculate the eigenstates and the spectrum of the system, and identify quantum breather states as weakly splitted tunneling pairs of states [27,28]. These eigenstates appear in the middle of the energy spectrum of the system and are characterized by correlations between the two junctions —if one of them is strongly excited, the other one is not, and vice versa. By exciting one of the junctions to a large energy, we strongly overlap with QB tunneling states. Consequently we trap the excitation on the initially excited junction on a time scale which sensitively depends on the amount of energy excited, and on the applied bias. We describe how this trapping could be experimentally observed in time using techniques for manipulating JJ qubits.

The system is sketched in fig. 1a: two JJs are coupled by a capacitance C_c , and they are biased by the same current I_b . The strength of the coupling due to the capacitor is $\zeta = C_c/(C_c + C_J)$. The Hamiltonian of the system is

$$H = \frac{P_1^2}{2m} + \frac{P_2^2}{2m} + U(\varphi_1) + U(\varphi_2) + \frac{\zeta}{m} P_1 P_2, \quad (2)$$

where

$$m = C_J(1 + \zeta) \left(\frac{\Phi_0}{2\pi} \right)^2, \quad (3)$$

$$P_{1,2} = (C_c + C_J) \left(\frac{\Phi_0}{2\pi} \right)^2 (\dot{\varphi}_{1,2} - \zeta \dot{\varphi}_{2,1}). \quad (4)$$

When the junctions are in the superconducting state, they behave like two coupled anharmonic oscillators. The plasma frequency is $\omega_p = \sqrt{2\pi I_c / \Phi_0 C_J (1 + \zeta)} [1 - \gamma^2]^{1/4}$, and $\gamma = I_b / I_c$ is the normalized bias current. The classical equations of motion of the system admit breather solutions [29], which are time periodic, and for which the energy is localized predominantly on one of the junctions (fig. 1c). These orbits are numerically computed with high accuracy by using Newton algorithms [30,31]. At the studied energies the classical phase space is mixed, and breathers are located inside regular islands, which are embedded in a chaotic layer.

In the quantum case we compute the energy eigenvalues and the eigenstates of the system. We neglect quantum escape for states which will not escape in the classical limit. Thus, we use a simple model for the single JJ, where the potential energy is changed by adding a hard wall which prevents escape:

$$U_q(\varphi) = \begin{cases} U(\varphi), & \text{if } \varphi \leq \pi - \varphi_0, \\ \infty, & \text{if } \varphi > \pi - \varphi_0, \end{cases} \quad (5)$$

where $\varphi_0 = \arcsin \gamma$ is the position of the minimum of the potential and $\pi - \varphi_0$ gives the position of the first maximum to the right from the equilibrium position φ_0 (fig. 1b). We will later compare the obtained tunneling times with the true state-dependent escape times.

The Hamiltonian of the two-junction system is given by $\hat{H} = \hat{H}_1 + \hat{H}_2 + \zeta \hat{V}$, where $\hat{H}_i = \hat{P}_i^2 / 2m + U_q(\hat{\varphi}_i)$ is the single-junction Hamiltonian and $\hat{V} = \hat{P}_1 \hat{P}_2 / m$ is the interaction that couples the junctions. The eigenvalues ε_{n_i} and eigenstates $|n_i\rangle$ of the single-junction Hamiltonian \hat{H}_i were computed by using the Fourier grid Hamiltonian method [32]. Note that $|n_i\rangle$ is also an eigenstate of the number operator \hat{n}_i with eigenvalue n_i . In the harmonic approximation $\hat{n}_i = \hat{a}_i^\dagger \hat{a}_i$, where \hat{a}_i^\dagger and \hat{a}_i are the bosonic creation and annihilation operators. Since only states with energies below the classical escape energy (barrier) are taken into account, the computed spectra have a finite upper bound. The perturbation \hat{V} does not conserve the total number of quanta $n_1 + n_2$, as seen from the dependence of the momentum operators on the bosonic creation and annihilation operators in the harmonic approximation: $\hat{P}_{1,2} = (\Phi_0 / 2\pi) \sqrt{(1 + \zeta) C_J \hbar \omega_p / 2} (\hat{a}_{1,2} - \hat{a}_{1,2}^\dagger) / i$.

The Hamiltonian matrix is written in the basis of product states of the single-junction problem $\{|n_1, n_2\rangle = |n_1\rangle \otimes |n_2\rangle\}$. The invariance of the Hamiltonian under permutation of the junction labels allows us to use symmetric and antisymmetric basis states,

$$|n_1, n_2\rangle_{S,A} = \frac{1}{\sqrt{2}} (|n_1, n_2\rangle \pm |n_2, n_1\rangle) \quad (6)$$

to reduce the full Hamiltonian matrix to two smaller symmetric and antisymmetric decompositions of \hat{H} , which after diagonalization respectively give the symmetric and antisymmetric eigenstates of the system.

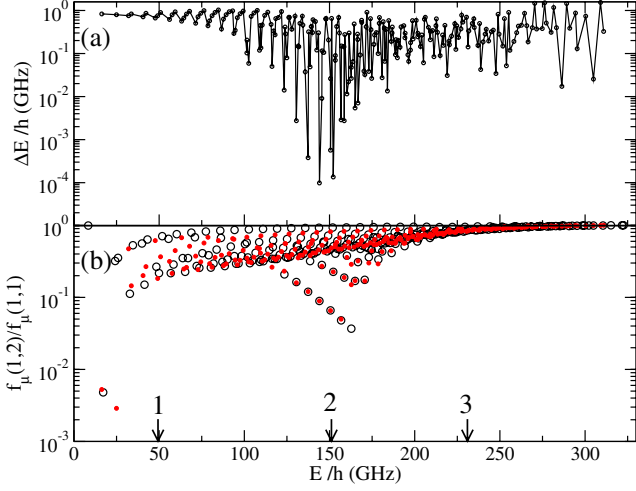


Fig. 2: (a) Energy splitting and (b) correlation function *vs.* energy for the two-junction system (open circles, symmetric eigenstates; filled circles, antisymmetric eigenstates). The labeled arrows mark the energy corresponding to the peak of the spectral intensity in figs. 3b, d, and f (see text). The parameters are $\gamma = 0.945$ and $\zeta = 0.1$ (22 levels per junction).

In order to identify quantum breather states, whose corresponding classical orbits are characterized by energy localization, we define the correlation functions:

$$f_{\mu}(1, 2) = \langle \hat{n}_1 \hat{n}_2 \rangle_{\mu}, \quad (7)$$

$$f_{\mu}(1, 1) = \langle \hat{n}_1^2 \rangle_{\mu}, \quad (8)$$

where $\langle \hat{A} \rangle_{\mu} = \langle \chi_{\mu} | \hat{A} | \chi_{\mu} \rangle$, $\{ | \chi_{\mu} \rangle \}$ being the set of eigenstates of the system. The ratio $0 \leq f_{\mu}(1, 2) / f_{\mu}(1, 1) \leq 1$ measures the site correlation of quanta: it is small when quanta are site correlated (when there are many quanta on one junction there are almost none on the other one) and close to unity otherwise.

In fig. 2 we show the nearest-neighbor energy spacing (splitting) and the correlation function of the eigenstates. For this, and all the rest, we used $I_c = 13.3 \mu\text{A}$, $C_J = 4.3 \text{pF}$, and $\zeta = 0.1$, which are typical values in experiments. We see that in the central part of the spectrum the energy splitting becomes small in comparison to the average. The corresponding pairs of eigenstates, which are tunneling pairs, are site correlated, and thus QBs. In these states many quanta are localized on one junction and the tunneling time of such an excitation from one junction to the other (given by the inverse energy splitting between the eigenstates of the pair) can be exponentially large and depends sensitively on the number of quanta excited.

The fact that the most site-correlated eigenstates occur in the central part of the energy spectrum may be easily explained as follows: Let N be the highest excited state in a single junction, with a corresponding maximum energy ΔU (fig. 1). For two junctions the energy of the system with both junctions in the N -th state is $2\Delta U$, which

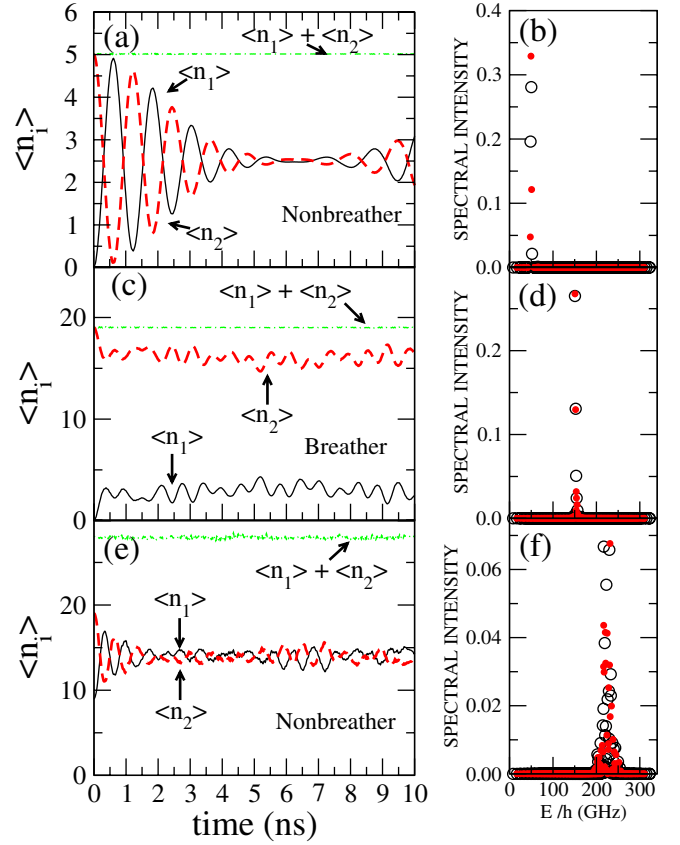


Fig. 3: Time evolution of expectation values of the number of quanta at each junction for different initial excitations and their corresponding spectral intensity. (a) and (b): $|\Psi_0\rangle = |0, 5\rangle$; (c) and (d): $|\Psi_0\rangle = |0, 19\rangle$; (e) and (f): $|\Psi_0\rangle = |9, 19\rangle$. Open circles, symmetric eigenstates; filled circles, antisymmetric eigenstates. The energies of the peaks in the spectral intensity are marked by labeled arrows in fig. 2b (see text). The parameters are $\gamma = 0.945$ and $\zeta = 0.1$ (22 levels per junction).

roughly is the width of the full spectrum. Thus, states of the form $|N, 0\rangle$ and $|0, N\rangle$ that have energy ΔU are located roughly in the middle.

With the eigenvalues and eigenstates we compute the time evolution of different initially localized excitations, and the expectation values of the number of quanta at each junction $\langle \hat{n}_i \rangle(t) = \langle \Psi(t) | \hat{n}_i | \Psi(t) \rangle$. Results are shown in figs. 3a, c, and e. Also we compute the spectral intensity $I_{\mu}^0 = |\langle \chi_{\mu} | \Psi_0 \rangle|^2$, which measures how strong the initial state $|\Psi_0\rangle$ overlaps with the eigenstates. Results are shown in figs. 3b, d, and f, where we can see a peak in each case, which corresponds to the arrows in fig. 2b. We can see that the initial state $|\Psi_0\rangle = |0, 5\rangle$ overlaps with site-correlated eigenstates with an energy splitting between them being relatively large and hence the tunneling time of the initially localized excitation is short. For the case $|\Psi_0\rangle = |0, 19\rangle$ QBs are excited: The excitation overlaps strongly with tunneling pairs of eigenstates in the central part of the spectrum, which are site correlated and nearly degenerate. The tunneling time of such an excitation is

very long, and thus keeps the quanta localized on their initial excitation site for corresponding times. Finally the initial state $|\Psi_0\rangle = |9, 19\rangle$ overlaps with weakly site-correlated eigenstates with large energy splitting. Hence the tunneling time is short.

We tested whether a (coherent or incoherent) spreading of the initial state over a suitable energy window affects the results discussed above. For instance instead of using the basis state $|0, 19\rangle$ as the initial state (figs. 3c, d), we superposed the basis states $|0, 20\rangle$, $|0, 19\rangle$, $|0, 18\rangle$, and $|0, 17\rangle$. We found that the results qualitatively do not change.

The experimental observation of QBs may be possible using the scheme of McDermott *et al.* for simultaneous state measurement of coupled Josephson phase qubits [6], where by applying current pulses the time evolution of the occupation probabilities in the qubits is measured. Applying a first microwave pulse on one of the junctions excites it into a high-energy single-junction state with energy ε_l and leaves the other one in the ground state. In this way we have an initial state similar to the ones shown in fig. 3. After a variable time period we apply simultaneous current pulses to the junctions to lower their energy barriers ΔU and enhance the probability of tunneling outside the potential well. Then we test which junction switches to the resistive state (detected by a measurable voltage across it). By repeating the measuring many times we obtain the populations in the junctions as a function of the time period between the initial pulse and the simultaneous measuring pulses.

Let us discuss the so far neglected quantum escape. For that we computed the escape time τ_{escape} by using the semiclassical formula [33]

$$\tau_{escape}^{-1}(\varepsilon) = \frac{\omega(\varepsilon)}{2\pi} \exp \left\{ -\frac{2}{\hbar} \int_a^b p(\varphi) d\varphi \right\}, \quad (9)$$

where a and b are the turning points of the classical motion in the reversed potential at $U(\varphi) = \varepsilon$, $p(\varphi) = \sqrt{2[U(\varphi) - \varepsilon]}$, and $\omega(\varepsilon)/2\pi$ is the frequency of the oscillations inside the initial well. In table 1 we show the escape time from different metastable states, and we compare it with the tunneling time τ_{tunnel} of an initial excitation $|\Psi(0)\rangle = |0, l\rangle$ between the two junctions, estimated from the energy splitting of the (symmetric-antisymmetric) pair of eigenstates with the largest overlap with the initial excitation. We see that for $l = 19$, where we excite QBs, the escape time is long enough for observing at least one tunneling exchange between the two junctions before escaping to the resistive state. Note that the cases $l = 18$ and 17 also excite QBs which would show even more tunneling exchanges before escaping. The case $l = 16$ does not excite QBs but eigenstates that, though having small energy splitting, do not show strong site correlation of quanta as in the previous cases. From these results we expect that escaping to the resistive state will not prevent from the experimental observation of QB excitations.

Table 1: Escape times for metastable states in a single JJ τ_{escape} estimated by formula (9), and tunneling time of the initial excitation $|\Psi(0)\rangle = |0, l\rangle$ between the two junctions τ_{tunnel} estimated from energy splittings.

l	τ_{tunnel} (ns)	τ_{escape} (ns)
20	348	42
19	1.8×10^3	3.5×10^3
18	10.16×10^3	503.2×10^3
17	2.3×10^3	71.2×10^6
16	366	1.62×10^9

Another phenomenon that was not taken into account in our quantum model is decoherence. To be able to observe tunneling between the junctions the coherence time has to be longer than the shortest tunneling time between the junctions, which is on the order of 1 ns in the cases shown in figs. 3a and e. In the experiment shown in [24] using a few levels per junction a coherence time on the same order was obtained. However, in the experiment in [6] the coherence time was about 25 ns, and more recently in [7] the coherence time was approximately 80 ns. We expect that further improvements in experiments [5] will give us longer coherence times.

Note that the above coherence times are shorter than the tunneling times of QB excitations (see table 1), hence decoherence is an effect that cannot be ignored if one wants to do a more realistic quantum description of the system. When exciting a JJ to a high-energy state, relaxation (over dephasing) is usually the main source of decoherence. We can make a crude estimation of the corresponding relaxation time T_1 by using $T_1 \simeq \hbar Q/\varepsilon_l$ (Q is the quality factor of the junctions), which holds for a harmonic potential [34,35]. For $l = 19, 18$ and 17 , ε_l/\hbar is around 150 GHz (see fig. 2b). For the JJs used in [5], Q is between 500 and 1000, which leads to a relaxation time between 3 ns and 6 ns. It is much smaller than the tunneling time of the QB excitations, therefore one would expect to see instead of tunneling, a freezing of the QBs on one of the junctions before they decohere due to relaxation.

One could obtain more feasible results by increasing the bias current in such a way that there are less energy levels in the junctions. With this, exciting a QB would need less energy, and the relaxation time becomes longer. The tunneling time of that QB excitation is shorter, and might be even shorter than the relaxation time, allowing one to observe tunneling before relaxation. This possibility, and the inclusion of decoherence in our model, are issues that will be addressed in a future work.

In summary, we have studied the classical and quantum dynamics of high-energy localized excitations in a system of two capacitively coupled JJs. In the classical case the equations of motion admit time periodic localized excitations (discrete breathers) which can be numerically computed. For the quantum case we showed that excitation of one of the junctions to a high level

leaving the other junction in the ground state leads to a QB with long tunneling time. This is possible because the excitation overlaps strongly with tunneling-pair eigenstates which live in the central part of the energy spectrum and localize energy on one of the junctions. This result would not qualitatively change if we excite a (coherent or incoherent) superposition of several product basis states instead of only one. We showed that with the available techniques for manipulating JJ qubits the experimental observation of QB excitations is possible. Escaping to the resistive state of the junctions (which together with decoherence was not taken into account in our quantum model) would not prevent us from doing that, and we expect that improvements in preparation (higher quality factors) and isolation techniques of JJ will lead to long enough coherence times, such that the phenomena we described in this work will be clearly observed. That would ultimately pave the way of a controlled stirring of quanta on networks of JJs.

This work was supported by the DFG (grant No. FL200/8) and by the ESF network-programme AQDJJ.

REFERENCES

- [1] LIKHAREV K. K., *Dynamics of Josephson Junctions and Circuits* (Gordon and Breach Science Publishers, Philadelphia) 1984.
- [2] LEGGETT A. *et al.* (Editor), *Quantum Computing and Quantum Bits in Mesoscopic Systems* (Kluwer Academic/Plenum Publishers, New York) 2004.
- [3] ESTEVE D. *et al.* (Editor), *Les Houches 2003, Quantum Entanglement and Information Processing* (Elsevier, Amsterdam) 2004.
- [4] MARTINIS J. M. *et al.*, *Phys. Rev. Lett.*, **55** (1985) 1543.
- [5] STEFFEN M. *et al.*, *Phys. Rev. Lett.*, **97** (2006) 050502.
- [6] MCDERMOTT R. *et al.*, *Science*, **307** (2005) 1299.
- [7] STEFFEN M. *et al.*, *Science*, **313** (2006) 1423.
- [8] GRAHAM R. *et al.*, *Phys. Rev. Lett.*, **67** (1991) 255.
- [9] MONTANGERO S. *et al.*, *Europhys. Lett.*, **71** (2005) 255.
- [10] POZZO E. N. *et al.*, *Phys. Rev. Lett.*, **98** (2007) 057006.
- [11] FLEUROV V., *Chaos*, **13** (2003) 676.
- [12] SCOTT A. C. *et al.*, *Physica D*, **78** (1994) 194.
- [13] WANG W. Z. *et al.*, *Phys. Rev. Lett.*, **76** (1996) 3598.
- [14] FILLAUX F. *et al.*, *Phys. Rev. B*, **42** (1990) 5990.
- [15] FILLAUX F. *et al.*, *Phys. Rev. B*, **58** (1998) 11416.
- [16] RICHTER L. J. *et al.*, *Phys. Rev. B*, **38** (1988) 10403.
- [17] GUYOT-SIONNEST P., *Phys. Rev. Lett.*, **67** (1991) 2323.
- [18] DAI D. J. *et al.*, *Surf. Sci.*, **312** (1994) 239.
- [19] CHIN R. P. *et al.*, *Europhys. Lett.*, **30** (1995) 399.
- [20] JAKOB P., *Phys. Rev. Lett.*, **77** (1996) 4229.
- [21] JAKOB P., *Appl. Phys. A: Mater. Sci. Process.*, **75** (2002) 45.
- [22] OKUYAMA H. *et al.*, *Phys. Rev. B*, **63** (2001) 233404.
- [23] EDLER J. *et al.*, *Phys. Rev. Lett.*, **93** (2004) 106405.
- [24] BERKLEY A. J. *et al.*, *Science*, **300** (2003) 1548.
- [25] JOHNSON P. R. *et al.*, *Phys. Rev. B*, **67** (2003) 020509(R).
- [26] BLAIS A. *et al.*, *Phys. Rev. Lett.*, **90** (2003) 127901.
- [27] FLACH S. *et al.*, *J. Phys.: Condens. Matter*, **9** (1997) 7039.
- [28] PINTO R. A. *et al.*, *Phys. Rev. A*, **73** (2006) 022717.
- [29] FLACH S. *et al.*, *Phys. Rep.*, **295** (1998) 181.
- [30] DAUXOIS T. *et al.* (Editor), *Energy Localization and Transfer* (World Scientific) 2004.
- [31] CHEN D. *et al.*, *Phys. Rev. Lett.*, **77** (1996) 4776.
- [32] CLAY MARSTON C. *et al.*, *J. Chem. Phys.*, **91** (1989) 3571.
- [33] LANDAU L. D. and LIFSHITZ E. M., *Quantum Mechanics* (Pergamon, London) 1958.
- [34] MARTINIS J. M. *et al.*, *Phys. Rev. B*, **35** (1987) 4682.
- [35] ESTEVE D. *et al.*, *Phys. Rev. B*, **34** (1986) 158.